Chapter

# Formulae of Sediment Transport in Unsteady Flows (Part 2)

*Shu-Qing Yang*




## Abstract

Sediment transport (ST) in unsteady flows is a complex phenomenon that the existing formulae are often invalid to predict. Almost all existing ST formulae assume that sediment transport can be fully determined by parameters in streamwise direction without parameters in vertical direction. Different from this assumption, this paper highlights the importance of vertical motion and the vertical velocity is suggested to represent the vertical motion. A connection between unsteadiness and vertical velocity is established. New formulae in unsteady flows have been developed from inception of sediment motion, sediment discharge to suspension's Rouse number. It is found that upward vertical velocity plays an important role for sediment transport, its temporal and spatial alternations are responsible for the phase lag phenomenon and bedform formation. Reasonable agreement between the measured and the proposed conceptual model was achieved.


**Keywords:** unsteady flow, shields number, rouse number, sediment transport, vertical velocity

## 1. Introduction

Sediment transport is the movement of solid particles driven by fluid like water or wind in rivers, lakes, reservoirs, coastal waters. Generally, in the real world the flow is unsteady like flood waves, tidal waves and wind waves, because steady and uniform flows are very rare in reality. Even so, it is understandable that sediment transport is first observed under well controlled conditions in laboratory, and then the data are collected to calibrate the models. These formulae are further examined using field data by assuming the laboratory flow conditions (generally steady and uniform flows) can be extended to rivers and coastal waters (generally unsteady and non-uniform).

In the literature, many formulae use the boundary shear stress $\tau$ (=$\rho ghS$) to express sediment discharge, like *Einstein* [1], *Meyer-Peter* and *Muller* [2], *Yalin* [3], *Engelund* and *Hansen* [4] and *Ackers and White* [5]. For example, the Meyer-Peter and Muller equation for the bed load and Engelund-Hansen formula for the total load have the following forms:

$$\frac{g_b}{\sqrt{\left(\rho_s/\rho - 1\right)gd_{50}}} = 8.0\left(\frac{\tau}{(\rho_s - \rho)gd_{50}} - 0.047\right)^{1.5} \tag{1}$$

$$c_f \frac{g_t}{\sqrt{\left(\rho_s/\rho - 1\right)gd_{50}}} = 0.1\left[\frac{\tau}{(\rho_s - \rho)gd_{50}}\right]^{5/2} \tag{2}$$

where $g_b$ and $g_t$ = bed-load and total load of sediment discharge per unit width, $g$ = gravitational acceleration, $d_{50}$ = median sediment size, $\rho_s$ = sediment density, and $\rho$ = water density, $h$ = water depth, $S$ = energy slope, $c_f$ = friction factor which is constant in fully rough regime. The subscribes $b$ and $t$ denote the bed load and the total load. Eqs. (1) and (2) demonstrate that if $d_{50}$, $\rho_s$ are constant, sediment discharge only depends on $\tau$.

Alternatively, the mean velocity $U$ was selected to represent the hydraulic parameter for sediment discharge or concentration like the *Velikanov*'s [6] parameter, $U^3/(gh\omega)$. The WIHEE's [7] equation which has been widely used in China has the following form:

$$C = k_1 \left(\frac{U^3}{gh\omega}\right)^m \tag{3}$$

where $C$ = sediment concentration, $k_1$ and $m$ are empirical coefficient, $\omega$ = sediment settling velocity.

Besides the parameters $U$ and $\tau$ alone, attempts have been made to correlate the sediment transport with the product of $U$ and $\tau$. Probably *Bagnold* [8] was the first one to do so, and it is known as the stream power (= $\tau U$). Likewise, the product of $U$ and $S$, or the unit stream power $US/\omega$ was used by *Yang* [9]. *van Rijn* [10] selected $u_*'$, the shear velocity related grains, in his equations, i.e., $T$, and $d_*$, they are

$$T = \frac{u_*'^2 - u^2{}_{*c}}{u^2_{*c}} \tag{4}$$

$$d_* = d\left[\frac{(\rho_s/\rho - 1)g}{\nu^2}\right]^{1/3} \tag{5}$$

where

$$u'_* = \frac{U}{2.5\ln\frac{11h}{2d_{50}}} \tag{6}$$

where the critical shear stress $\tau_c = \rho u_{*c}^2$, $\nu$ = kinematic viscosity.

*Yang and Tan* [11] found that the shear velocity $u_*'$ is responsible for transporting the sediment particles, *Yang* [12] defined the energy dissipation on sediment transport as $E = \tau u_*'$, and obtained the formula of sediment transport:

$$\overrightarrow{g_t} = \left(\frac{\rho_s}{\rho_s - \rho}\right) k \overrightarrow{u'_*} \left(\frac{E - E_c}{\omega}\right) \tag{7}$$

where the arrows represent the direction, i.e., sediment is transported in the same direction as the near bed flow if the flow directions of upper and lower layers are different, $E_c$ (= $\rho u_{*c}^3$), $k$ is a constant (= 12.2) and insensitive to other hydraulic parameters like Froude number, Reynolds number, relative roughness and Rouse number [13].

Obviously, the hypothesis in all equations listed above is that the higher the streamwise parameters are (e.g., $U$, $u_*'$, $\tau$, $E$ or $US$ etc.), the more particles are transported [14]. However, this prediction is invalid in unsteady conditions [15, 16]. Tabarestani and Zarrati [17] reviewed the performance of existing formulae and concluded that in general, the sediment discharge under unsteady flow conditions cannot be predicted by these equations, because the streamwise parameters in the rising limb is much larger than that in the falling limb, but the measured sediment load yield during hydrograph rising limb is smaller than that in the falling limb. The highest $g_t$ or $C$ comes after the peak flowrate or velocity $U$, and the lag phenomenon has been widely observed and reported. The shear stress based theory has also been questioned by *Nelson et al.* [16] who observed from their experiment that the sediment flux increases even though the bed shear stress decreases.

*Sleath* [18] argued that when the "pressure gradient" is not small compared with the shear stress exerted by the flow, these equations need to be modified and a new $S_1$ n*umber* should be considerd for wave conditions, its definition is:

$$S_1 = \frac{\rho U \sigma}{(\rho_s - \rho)g} \tag{8}$$

where $\sigma$ is the angular frequency of waves.

Alternatively Francalanci et al. [19] suggest using the pressure $P$ to express the unsteadiness, but Liu and Chiew [14] and Cheng and Chiew [20] use the hydraulic gradient $i$ in the sediment layer. The challenge also comes from the bursting phenomenon even in steady and uniform flows. It is found that the similar lag phenomenon exists in a bursting cycle [21, 22]. *Cellino and Lemmin's* [23] experiments demonstrate that the upward flow (or ejection) appears responsible for the threshold of particle movement, the entrainment and transport of bedload and lifting of sediment into suspension. This cannot be explained by the parameters of pressure $P$ or hydraulic gradient $i$ or seepage velocity.

It seems that there is a knowledge gap between the unsteady flows and sediment transport, a new parameter is needed to be developed to express the unsteadiness, thus the above phenomena can be explained. In this study, the induced vertical velocity $V$ is selected to express the effect of unsteadiness on the sediment, an attempt is made to justify its suitability for sediment transport as well as the phenomena of phase-lag and bedform formation. The research objectives include:

1. to compare $V$ with other parameters to express the force induced by unsteady flows;

2. to establish a simple connection between $V_b$ in the sediment layer and $V$ in the main flow;

3. to develop formulae to express critical shear stress, sediment discharge and Rouse number in unsteady flows;

4. to explain the mechanism of phase lags and bedform formation.

The chapter discusses the existence of vertical velocity in unsteady flows first, then the influence of vertical velocity on critical shear stress of sediment is analyzed, followed by its influence on sediment discharge and suspension concentration. Finally a comprehensive discussion is provided.

## 2. Theoretical consideration

Sediment transport is a joint result of streamwise and vertical motions of fluid. This joint effect can be seen from the definition of Shields number that is the ratio of forces in streamwise and vertical directions as noted by *Francalanci et al*. [19]:

$$\tau_* = \frac{\tau}{(\rho_s - \rho)gd} \tag{9}$$

where $\tau_*$ = Shields number. The numerator denotes the streamwise friction force and the denominator represents the vertical force, i.e., the net buoyant force of particle. Sediment starts to move at $\tau_* \geq \tau_{*c}$, the critical Shields number.

A simple wave model is shown in **Figure 1a** where a surface wave induces a vertical motion for the particles on the permeable bed. The surface wave is propagating in the research domain where the current velocity is $U$, the streamwise parameters like the point velocity, shear stress, pressure $P$ and hydraulic gradient $i$ in the soil are also modified. In this study, the induced vertical motion has been expressed by velocity at the interface is $V_b$. The relationship between the wave and its induced vertical velocity is shown in **Figure 1b**.

In **Figure 1**, the continuity equation of unsteady flows must be satisfied, i.e.,

$$\frac{\partial u}{\partial x} + \frac{\partial v}{\partial y} = 0 \tag{10}$$

where $u$ and $v$ are the streamwise and vertical time-averaged velocities in $x$ and $y$ directions. The vertical velocity can be determined from Eq. (10) as follows:

$$v = -\int \frac{\partial u}{\partial x} dy \tag{11}$$

In Eq. (11) the term $\partial u/\partial x$ is the gradient of streamwise velocity in $x$-direction, it is positive if the velocity becomes higher to downstream (accelerating), and

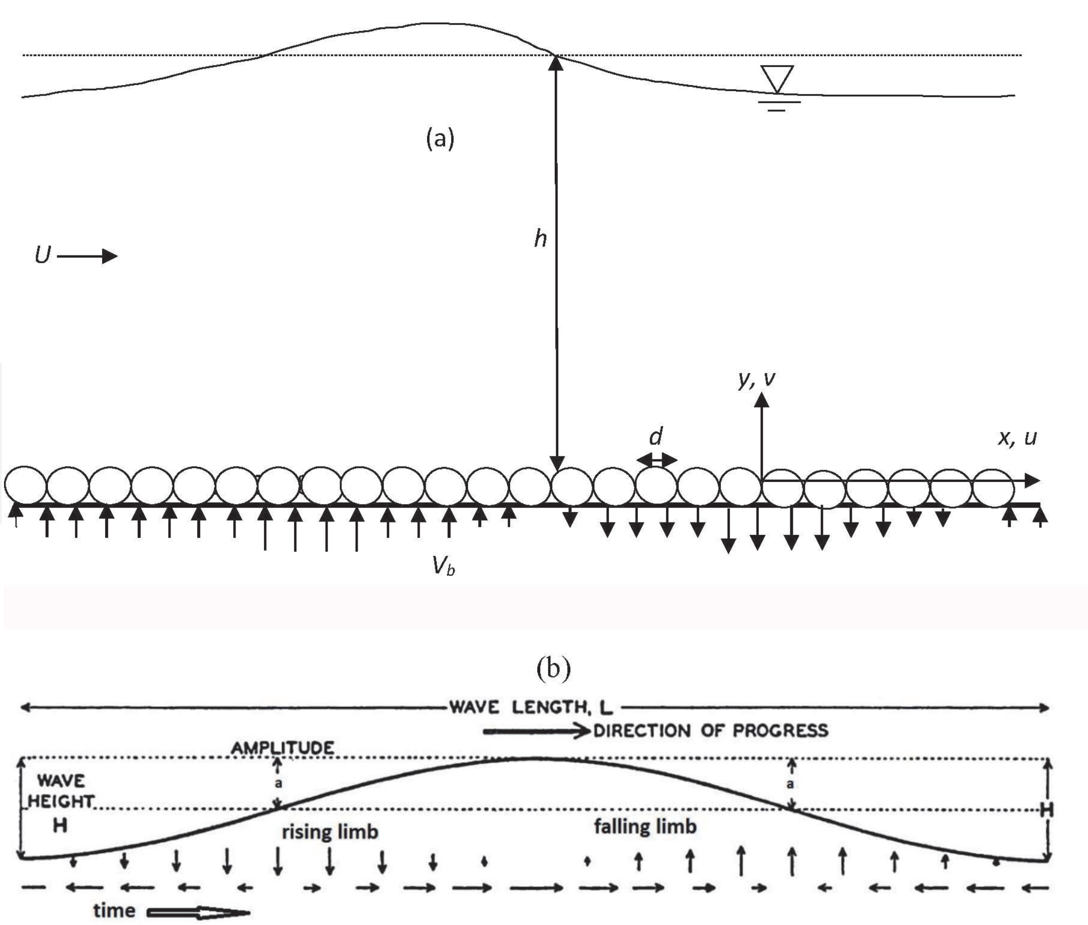


**Figure 1.**
*(a) Schematic diagrams showing interaction of surface waves and induced and vertical motions at the sediment layer along x direction. (b) Definition of progressive wave and its induced vertical velocity at different time (x = constant).*

negative if the fluid particles experience decelerating. Hence, the accelerating flow yields a negative or downward $v$, the decelerating flow generates an upward or positive $v$.

At the permeable boundary, the fluid velocity must meet the continuous boundary condition, i.e., $v_{(y=0^+)} = v_{(y=0^-)}$, or the velocity inside the sediment layer must be same as the velocity in the main flow at the interface. Thus it can be concluded that a downward velocity exists in the sediment layer when the main flow layer is accelerating, and an upward velocity appears when a flow is decelerating.

Generally speaking, the rising limb is the accelerating stage which induces a downward velocity, but the decelerating stage in ebb limb generates an upward velocity. In the real world, it is also possible that flows in both rising/falling limbs are accelerated as observed by *Song and Graf* [24], who used acoustic Doppler velocity profiles measured the vertical velocity in unsteady open channel flows, and found during the rising/falling limbs, "the measured vertical velocity are almost always negative, and this implies that the flows of the present experiments are accelerating ones". On the other hand, *Leng and Chanson* [25] used an acoustic Doppler velocimeter (ADV) measured the vertical velocity in tidal bores and found that the vertical velocity is always upward or decelerating in both rising and falling limbs. To simplify the discussion, this study only discusses the cases shown in **Figure 1b** and the waves' influence on parameters like $q$, $U$ is assumed to be negligible.

The direction of vertical velocity can noticeably change the profile of Reynolds shear stress, streamwise velocity etc. [12, 26]. One of the examples is shown in **Figure 2**, *Kemp and Simons* [27, 28] measured the velocity profiles in a flume where the incident wave was set to propagate against or along the direction of the currents. The flow depth at the test section was kept at 200 mm for all tests. Regular waves were generated with a constant wave period of 1 second. The wave heights were 27.9 to 20.7 mm, the wave lengths were 1053 mm to 1426, respectively. Their results clearly show that the measured velocity is greater than log-law's prediction when waves opposite the current as the original uniform flow is decelerated by the waves from downstream, but less than the log-law's prediction when the waves to the currents as the original uniform flow is accelerated by waves from upstream. Existing research [26, 29] shows that in a turbulent flow the log-law is satisfied if the upward velocity in the main flow $V = 0$, but the measured velocity is higher than the log-law's prediction if $V > 0$ or upward velocity exists, and the maximum velocity is submerged if $V < 0$ (or downward velocity exists). Further investigation shows that a decelerating flow generates an upward velocity, but an accelerating

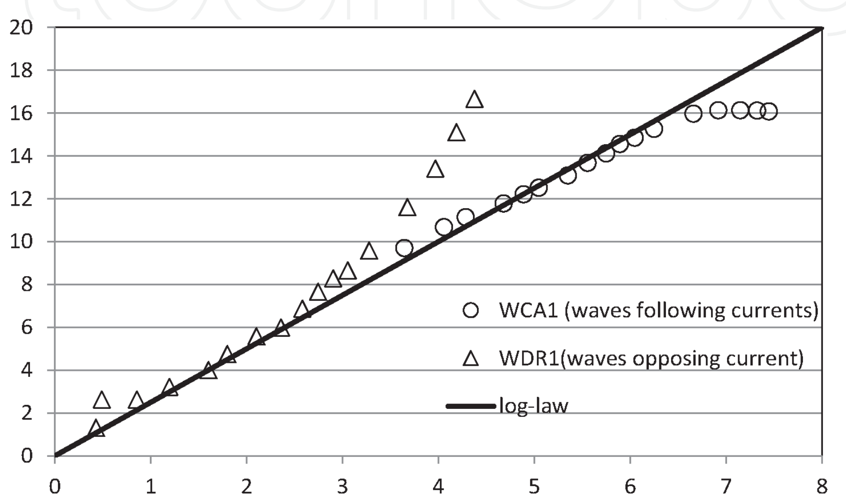


**Figure 2.**
*Deviation of measured velocity from log-law by Kemp and Simons [21, 22].*

flow induces downward velocity [30]. Therefore one can infer that in **Figure 2**, there exists an upward velocity for waves against a current or the waves make the current decelerated; but a downward velocity exists in the case of waves following current, which accelerates the water.

For sediment particles in **Figure 1**, the settling velocity $\omega$ in still water is determined by:

$$C_d \pi \frac{d^2}{4} \frac{\rho \omega^2}{2} = \pi \frac{d^3}{6} g(\rho_s - \rho) \tag{12}$$

where drag coefficient $C_d$ depends on the Reynolds number Re (= $\omega d/\nu$) and $C_d$ = 0.45 for large Reynolds number, i.e., Re >1000.

If a surface wave induces an upward velocity $V_s$ in the preamble sediment layer, the net settling velocity is reduced to $\omega$ - $V_b$. The reduction of settling velocity could be treated by altering its density from $\rho_s$ to $\rho_s$' by assuming the particle's size remains unchanged, and the force balance equation is similar to Eq. (12) with the following form:

$$C_d' \pi \frac{d^2}{4} \frac{\rho(\omega - V_b)^2}{2} = \pi \frac{d^3}{6} g(\rho_s' - \rho) \tag{13}$$

From Eqs. (12) and (13), one can derive the following relationship:

$$\frac{\rho_s' - \rho}{\rho_s - \rho} = \alpha \left(1 - \frac{V_b}{\omega}\right)^2 \tag{14}$$

where $\alpha = C_d'/C_d$ and $\alpha$ = 1 are assumed to simplify the mathematical treatment. Eq. (14) shows that if $V_b$ is upward, then $\rho_s' < \rho_s$, or the sediment particles become lighter in the "boiling" environment. If the upward $V_b$ = ω, Eq. (14) shows that the sediment density is similar to the water density $\rho_s' = \rho$. If the sediment particles are exercising the downward velocity (negative $V_b$), then the density $\rho_s' > \rho_s$, or the sediment behaves like heavy metals. As the decelerating velocity can generate upward velocity, it can be inferred that if the streamwise parameters keep almost unchanged, the sediment can be more easily transported in decelerating flows relative to the accelerating flows. In other words, the sediment particles become lighter in decelerating flows (or decelerating phase), but heavier in accelerating flows/phase. As Eq. (10) is also valid for turbulent velocity and wave conditions, then the conclusion can be extended to the bursting phenomenon or wave conditions where the accelerating/decelerating phases alternate randomly or regularly, thus these equations provide a general tool to analyze sediment transport.

## 3. Influence of unsteadiness on critical shear stress for incipient sediment transport

It is interesting to discuss how the waves affect the initiation of sediment movement. For an unsteady flow, the existing Shields diagram may be invalid to express the threshold sediment motion, due to the existence of vertical velocity caused by its unsteadiness. When the apparent sediment density is included in the Shields number, it has the following form:

$$\tau'_* = \frac{\tau_c'}{(\rho_s' - \rho) g d} \tag{15}$$

where $\tau_c$' is the critical shear stress with vertical velocity. Inserting Eq. (14) into Eq. (15), one has:

$$\tau'_* = \frac{\tau'_c}{(\rho_s - \rho)gd}\left(\frac{\omega}{\omega - V_b}\right)^2 \tag{16}$$

Using Eq. (9), Eq. (16) can be rewritten as follows

$$\frac{\tau'_*}{\tau_*} = \left(\frac{\omega}{\omega - V_b}\right)^2 \tag{17}$$

Eqs. (16) and (17) generally express the relationship between the Shields number $\tau_*$' with waves and the original Shields number $\tau_*$ without waves. It predicts that the original Shields number may significantly deviate from the Shields curve subject to wave conditions.

Eq. (15) includes the influence of the vertical velocity, it demonstrates that the upward velocity reduces particles' apparent density, thus the required critical shear stress will be also reduced. Whilst the downward velocity increases the apparent density, thus the required critical shear stress is higher. If the cases with/without vertical velocity are compared, the critical shear stress without waves $\tau_c$ and the critical shear stress with waves $\tau_c$' have the following relationship:

$$\frac{\tau'_c}{\tau_c} = (1 - Y)^2 \tag{18}$$

and

$$Y = \frac{V_b}{\omega} \tag{19}$$

Eq. (18) shows that the critical shear stress $\tau_c$' in unsteady flows. It should be stressed that for sediment incipient motion, $V_b$ in Eq. (19) depends on the instantaneous maximum upward velocity for which the ejection of burst phenomenon, unsteadiness and others may jointly contribute. For flows shown in **Figure 2**, one can infer that the measured $\tau_c$' is less than Shields diagram's prediction when the waves propagate against the current, but the $\tau_c$' becomes larger than $\tau_c$ when the waves propagate with the current. The reason is that, the former generates an upward velocity in the decelerating flows, but the latter has a downward as it is an accelerating flow.

If the influence of small wave on the shear stress is negligible, the $Y$ with small waves must be higher than the $Y$ without waves. In such case, one can easily conclude from Eq. (18) that the $\tau_c$' (with waves) must be always less than $\tau_c$ (without waves). In the literature, it seems that many researchers agree that the existing Shields diagram can be extended to the wave-current motion (i.e., [31, 32]). Till recently, few researchers like *Green and MacDonald* [33] found waves, not currents initiate sediment transport, their data show that "observed $\tau_*$' never exceeded the theoretical dimensionless $\tau_*$". It is well known that for large particles, the critical Shields number $\tau_*$ = 0.06. They observed suspension at the same value of $\tau_*$ when waves are present in tidal flows, similar observations were reported by *Green and Coco* [34]. All of these observations can be easily explained by Eq. (18) when $Y \approx 1$.

It should be stressed that accelerating flows constrain sediment mobility from vertical point of view, but the higher velocity and shear stress in the rising limb

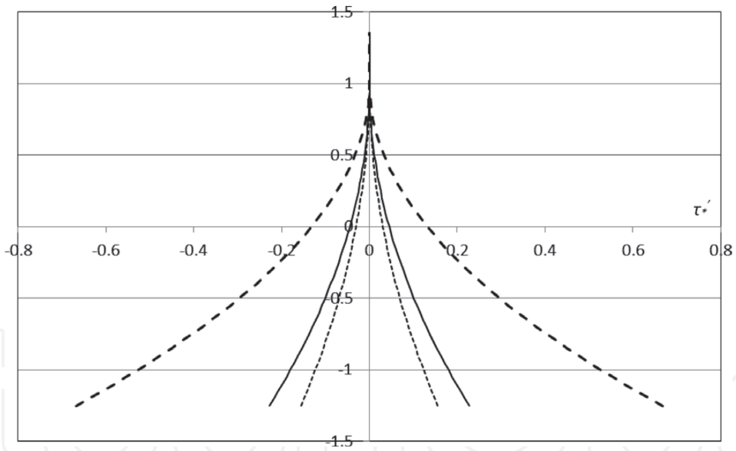


**Figure 3.**
*Sediment incipient conditions in wave conditions, the required shields numbers depend on the veritocal motion, i.e., ±Y. based on Eq. (15), the calculated solid line (——) represents non-cohesive sediment in shields diagram τ*' = 0.045; the dotted line (········) for τ*' = 0.03; and the dashed line (– –) for very fine sediment with τ*' = 0.13. Below these curves, particles remain static, above the curves particles are in mobile state.*

promote sediment transport in the streamwise direction, therefore the complete effect of accelerating flows in the rising limb should include both shear stress and maximum $Y$. Likewise, the decelerating flow makes particles "lighter" in vertical direction, but the reduced shear stress makes particles to move "harder". Therefore, one need to justify the critical shear stress by considering both streamwise and vertical parameters.

Eq. (18) clearly demonstrates that the critical shear stress is jointly determined by the streamwise and vertical motions. The coexistence of streamwise/vertical motions results in the invalidity of Shields diagram which can be improved by Eq. (18) and shown in **Figure 3**, where the Shields number in the original Shields diagram is $\tau_*$ = 0.045, 0.03 and 0.13 are calculated using Eq. (18). The region below the curves represents that the sediment is static, and above these curves is mobile. The calculated results show that when $Y \geq 0.7$, the sediment is mobile, for which the required shear stress is always zero.

## 4. Effects of vertical velocity induced by waves on sediment transport

As mentioned before that sediment transport is a joint effect of streamwise and vertical motions, the latter can be represented by the apparent sediment density. Therefore, Eq. (7) can be modified with the following way:

$$\vec{g_t} = \left(\frac{\rho_s'}{\rho_s' - \rho}\right) k \overrightarrow{u'_*} \left(\frac{E - E_c}{\omega - V_b}\right) \tag{20}$$

For sediment transport in waves conditions, the bed shear stress $\tau = \tau_w + \tau_{cu}$ and near bed velocity $u_b = u_w + u_{cu}$, where the subscripts w and cu refers to waves and currents. Yang [12] obtained the formula which agrees reasonably well with von Rijn's data in 1993, 1995 and 1999 for sediment transport when waves follow or oppose the currents, there are some angles between the direction of wave propagation and current, and waves are broken over a near shore bar, respectively. Even the best agreement has been achieved among the existing formulae, noticeable discrepancies imply that some mechanism of sediment transport by waves needs further investigations.

Eq. (20) shows that the direction of sediment motion is always the same as the near bed velocity. This is meaningful to specify the sediment moving direction in coastal waters where the direction of flow in up layer is often different from that in the bottom layer. Eq. (20) has the following simplified form [35]:

$$g_t = k\frac{\rho_s'}{\rho_s' - \rho}\tau_o\frac{u_*'^2 - u_{*c}'^2}{\omega'} \tag{21}$$

Inserting Eq. (12) into Eq. (21), one has:

$$g_t(Y) = k\left[\frac{\rho}{\rho_s - \rho}\left(\frac{1}{1-Y}\right)^2 + 1\right]\tau_o\frac{u_*'^2 - u_{*c}'^2}{\omega(1-Y)} \tag{22}$$

Eq. (22) shows that sediment transport rate is jointly determined by the streamwise flow conditions (i.e., $\tau_o$ and $u_*$') and $Y$.

For the maximum over-the-wave-cycle horizontal wave-orbital speed at the bed $U_b$ can be expressed by the wave height $H$ and the wave period $T$, as both these govern the wave-orbital speed at the bed at any given water depth $h$. For linear waves, this is expressed as

$$U_b = \frac{\pi H}{T\sinh(k_o h)} \tag{23}$$

where the dispersion relationship gives:

$$\sigma^2 = gk_o\tanh(k_o h) \tag{24}$$

$\sigma = 2\pi/T$, $k_o$ is the wave number and $k_o = 2\pi/L$, $L$ = wave length.

It can be assumed that at the interfacial boundary, $v(y = 0^+)$ has the same magnitude order as $U_b$, and the vertical velocity at the sediment layer can be expressed as

$$V_b = \beta U_b \tag{25}$$

To evaluate the influence of vertical velocity on sediment transport rate, one can compare the sediment transport rate in two cases: with or without the vertical velocity induced by waves if $\tau_o$ remain unchanged. At $V_b = 0$, Eq. (22) becomes:

$$g_t(0) = k\frac{\rho_s}{\rho_s - \rho}\tau_o\frac{u_*'^2 - u_{*c}'^2}{\omega} \tag{26}$$

From Eqs. (22) and (26), one has:

$$\frac{g_t(Y)}{g_t(0)} = \frac{\rho}{\rho_s(1-Y)^3} + \frac{\rho_s - \rho}{\rho_s(1-Y)} \tag{27}$$

where $g_t = Cq$ and $C$ = sediment concentration. For a current with very small waves, the influence of small waves on the discharge $q$ is negligible, thus $g_t(Y)/g_t(0) \approx C(Y)/C(0)$.

*Green* [36] measured sediment concentration in an estuarine intertidal flat in New Zealand under very small waves. The wave height is less than 10 cm, and wave period ranges from 1.0–1.8 s. The measured data shows that sediment concentration in the rising tide is not very high, the highest concentration is always appear in the ebb tide. Eq. (11) may provide an explanation when the rising tide is assumed to be accelerating and the falling tide is decelerating. A downward velocity is generated

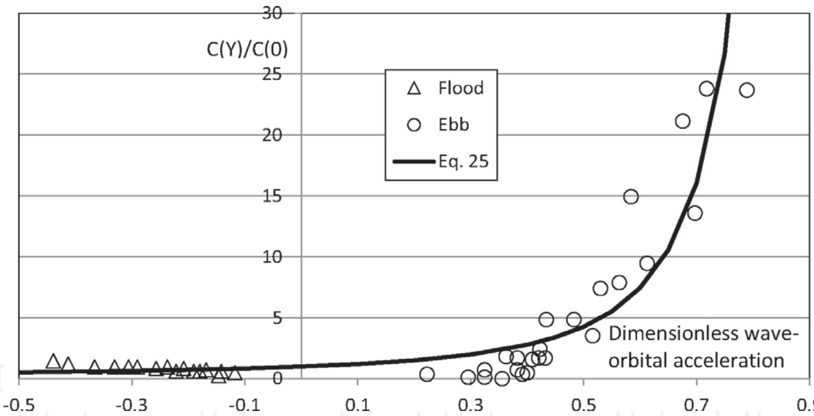


**Figure 4.**
*Measured sediment concentration normalized by C(0) = 5 mg/L versus the wave-orbital acceleration normalized by 23 cm/s². The raw data were deprived from Green [17], the acceleration in flood limb was set to negative and the acceleration in ebb stage was set to be positive. After this transformation, the obtained data can structurally match Eq. (27), implying the connection between the dimensionless parameters Y and the wave-orbital acceleration.*

the rising tide, which has the same effect on sediment as the particle's density becomes heavier. But during the falling limb or low tide, the particles become lighter, so the concentration becomes higher in this stage as shown in **Figure 4**.

In their analysis, *Green* [36] found that the "wave-plus-current-stress" theory provides poor agreement with their data. But the "wave-orbital speed" theory performed the best at predicting the incipient motion and suspension. They found a strong relationship between the measured sediment concentration and the wave-orbital acceleration $a_0$ which is defined as:

$$a_0 = \frac{1}{n}\sum_{i=1}^{n} \left(|U_{ZDC+}| - |U_{ZDC-}|\right)_i / T_{ZDCi} \tag{28}$$

where n = the number of zero-down crossing waves in the burst, $U_{ZDC+}$ is the maximum zero-down crossing current excursion in the positive direction from its average velocity. $U_{ZDC-}$ is the maximum zero-down crossing current excursion from the mean velocity in the negative direction, $T_{ZDC}$ is the period for the events.

**Figure 4** shows a plot $C(Y)/C(0)$ versus $Y$ ($=a_0/23$). *Green* [36] plotted his measured concentration in mg/L against $a_0$ using Eq. (28), in which the wave period is almost constant, thus the acceleration $a_0$ in Eq. (28) is actually the velocity. In **Figure 4**, the averaged concentration in the flood stage is used as $C(0)$ and $C(0)$ = 5 mg/L. It is found that data points match Eq. (27) very well when the acceleration $a_0$ is normalized by 23 cm/s$^2$ that is not clear the reason. In the calculation, the sediment and seawater densities are 2650 and 1025 kg/m$^3$, respectively.

It can be seen that the sediment transport rate can be significantly promoted by an ebb tide, if the upward velocity is 75% of settling velocity ($Y$ = 0.75), then the predicted sediment transport rate can be increased to 27 times of $g_t(0)$. **Figure 4** also shows that the sediment transport rate is slightly reduced if a downward flow exists. If $Y = -0.5$, then the sediment transport rate will be reduced to 1/2 of $g_t(0)$, this transport rate is achieved as the particles becomes "heavier".

## 5. Sediment suspension by tidal waves

The governing equation of suspended concentration can be derived from the continuity equation of solid-phase in the following form [37].

$$\frac{\partial c}{\partial t} = \frac{\partial\left(cu + \overline{c'u'}\right)}{\partial x} + \frac{\partial\left(cv + \overline{c'v'} - c\omega\right)}{\partial y} + \frac{\partial\left(cw + \overline{c'w'}\right)}{\partial z} \tag{29}$$

where c' = fluctuation of sediment concentration; $c$ = local time-averaged sediment concentration, $u$, $v$ and $w$ are the streamwise, vertical and lateral time-averaged velocities; $u'$, $v'$ and $w'$ are the velocity fluctuations in $y$ and $z$ directions, respectively.

In equilibrium conditions, time averaging of Eq. (29) gives:

$$\frac{\partial\left(cv + \overline{c'v'} - c\omega\right)}{\partial y} = 0 \tag{30}$$

The integration of Eq. (30) with respect to $y$ yields the following equation

$$cv + \overline{c'v'} - c\omega = 0 \tag{31}$$

If the eddy viscosity is used and Rouse number in Rouse's law has the following form:

$$Z(Y) = \frac{\omega(1 - Y)}{\kappa u_*} \tag{32}$$

$$\frac{Z(Y)}{Z(0)} = 1 - Y \tag{33}$$

Similar to the Shields number, many researchers also found that the measured Z is different from the calculated *Z. van Rijn* [10] and *Van de Graaff* [38] attribute this invalidity to sediment characteristics like size or streamwise flow strength, Eq. (33) indicates that if the vertical velocity exists, it also leads to the invalidity of Rouse number in practice.

*Rosea and Thorneb* [39] observed the Rouse number by measuring suspended sediment concentration profiles in the river Taw estuary, UK, where the flow is dominated by strong rectilinear, turbulent tidal currents. Their measurement was focused on the rising (flood) tide for a period of 3 hours. The measured $Z(Y)/Z(0)$ is shown in **Figure 5**, at the at the starting point the minimum vertical velocity $Y$ can be expected, and $Z(Y)/Z(0) \approx 1$ is observed, in the process, the streamwise velocity or shear velocity changed in a range of $\pm 20\%$, but the observed $Z(Y)/Z(0)$

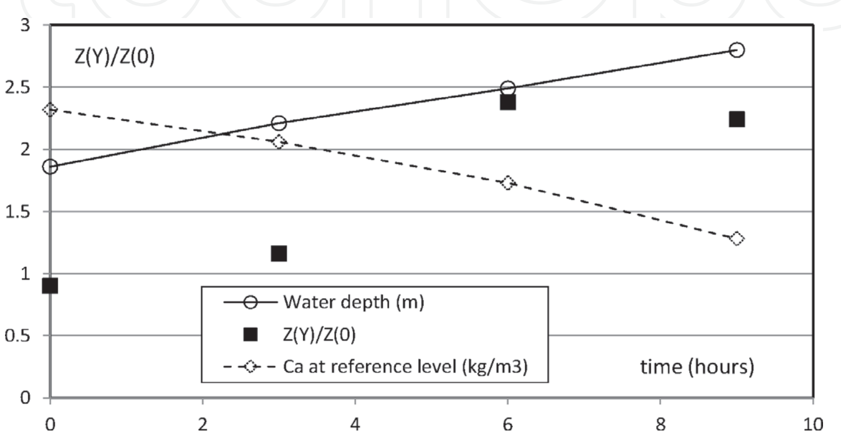


**Figure 5.**
*Measured Z(Y)/Z(0) in a rising tidal flow by Rose and Thome, at the starting point the streamwise velocity was the highest, minimum vertical velocity Y can be inferred, and Z(Y)/Z(0) ≈ 1 is observed and all data points show Z(Y)/Z(0) >1 in the rising tidal flow.*

| Profile | 1 | 2 | 3 | 4 | 5 | 6 | 7 | 8 | 1 | 2 | 3 | 5 |
|---|---|---|---|---|---|---|---|---|---|---|---|---|
| Tide | | | ebb | | | | | | Flood | | | |
| Rouse number | 0.55 | 0.45 | 0.45 | 0.50 | 0.27 | 0.35 | 0.48 | 0.50 | 0.68 | 0.95 | 0.7 | 1.2 |
| Average | | | 0.44 | | | | | | 0.70 | | | |

**Table 1.**
*Measured rouse numbers ($\omega/\kappa u_*$) in flood-tide and ebb tide by AL-Ragum [3].*

increased 150% and all data points shows that $Z(Y)/Z(0)$ >1 in the rising tidal flow, this is agreed with Eq. (33), i.e., accelerating flows generate an downward velocity or negative $Y$ that constrains sediment transport. This also can be seen from the measured sediment concentration $Ca$ at the reference level near the sea bed, the decreasing $Ca$ implies that the downward velocity makes the particles "heavier" to move, consequently $Ca$ is reduced to 44.8% of its original value.

If $Z(Y)/Z(0)$ in flood tide is compared with its values observed during ebb-tidal, Eq. (33) clearly indicates that the ebb-tide will have a lower value. This is in agreement with *Al-Ragum's* [40] observation as shown in **Table 1**. The data were collected from the Biscay Bay near Spain and France border. "The Rouse parameter varied with the tide, and the values were higher on the flood-tide than on the ebb-tide" as claimed by the author. The average Rouse parameter during flood tide is about 0.7, but it is reduced to 0.44 during the ebb tide. The flood tide generates 60% higher Rouse number relative to that during the ebb-tide.

## 6. Discussion on vertical velocity induced by unsteadiness and its effects

### 6.1 Unsteadiness parameter

For sediment transport by either flood waves in rivers or tidal waves in the sea, the unsteadiness plays a significantly role for sediment transport. The equations developed from steady flow may be invalid in unsteady flows. Some researchers like *Graf and Suszka* [41] found that the measured sediment transport rate in an unsteady flow is always larger than these equations' predictions. An unsteadiness parameter was proposed by them:

$$P_1 = \frac{h_p - h_1}{t_d u_*} \tag{34}$$

where $t_d$ is the duration of a hydrograph, $h_1$ is the initial or baseflow depth, $h_p$ is the peak flow depth of the hydrograph.

It is interesting to note that $(h_p\text{-}h_1)/t_d$ is actually the averaged vertical velocity $V$. Eq. (34) can be understood as the ratio of vertical velocity to the shear velocity, similar to $Y$ in Eq. (19). The unsteadiness parameter $P_1$ is useful for the prediction of time average sediment transport rate, but it cannot be used to explain the measured instantaneous rate $g_t$ or concentration $C$ that depends on the instantaneous vertical velocity, thus Eq. (19) may have a wider application. Compared with Eq. (34), Eq. (19) is simple and direct, the difficult parameter $u_*$ is replaced with the sediment settling velocity $\omega$ that is independent of flow characteristics, and the instantaneous vertical velocity $V$ can easily explain the observed phenomena in unsteady flows.

In fact, the unsteadiness parameter $S_1$ in Eq. (34) can be written in its alternative form:

$$S_1 = \frac{V}{(\rho_s/\rho - 1)ga/U} \tag{35}$$

where $a$ is the wave amplitude similar to $h_p$-$h_1$ in Eq. (34) and the vertical velocity $V = a\sigma/(2\pi)$, thus Eq. (35) shows that $S_1$ is similar to $Y$. *Sleath* [18] also proposed another parameter to express sediment transport by waves, i.e., $\omega/\sigma\delta$, and $\delta$ is the maximum thickness of the mobile layer, which can be read as $1/Y$ if $V_b = \sigma\delta$ is assumed.

**Figures 4** and **5** show the influence of unsteadiness on sediment transport in tidal flows. For flood waves in a river, *Lee et al.* [15] measured the transport rate over a series of triangular hydrographs. Their experimental results show the existence of phase lag between the peak discharge and peak sediment rate $g_t$, which lag is very long and about 6–15% of the flow hydrograph duration. **Figure 6** shows the hydrograph and measured sediment discharged by Lee et al. [15], it shows that the highest sediment transport rate appears in the falling stage when the shear stress is much less than that in the rising stage. This phase-lag phenomenon cannot be explained by those shown in Eqs. (1)–(7). It is interesting to note that there are two $g_t$ peaks in **Figure 6**, the mechanisms may be totally different, the former in the rising limb is likely generated by very high $\tau$ in the rising limb, but the upward velocity probably dominates the second peak where the shear stress is very small.

It should be mentioned that the peak sediment discharge in the rising limb is not always discernible as shown in **Figure 6**. For example, *Qi et al.* [42] reported that in Yellow River, artificial flood waves have been used to flush sediment in lower course of Yellow River by releasing water from its Xiaolangdi reservoir. As shown in **Figure 7**, the rising limb did not increase sediment concentration much, but the falling stage generated very high sediment concentration. From their experience, to enhance the flush efficiency, the duration of rising limb should be short as its rising flow does not increase $g_t$ or $C$ too much.

To interpret the results in **Figures 6** and **7**, the conceptual mathematical model in Eq. (27) may be useful as it covers the parameters in streamwise and vertical directions. Eq. (27) precisely suggests that the upward velocity may be responsible for the widely observed "phase lag" in sediment transport in rivers.

## 6.2 Mechanism of bedform formation

The formation of ripples and dunes over a flat mobile bed is an amazing phenomenon, and has attracted many investigations. All previous equations of

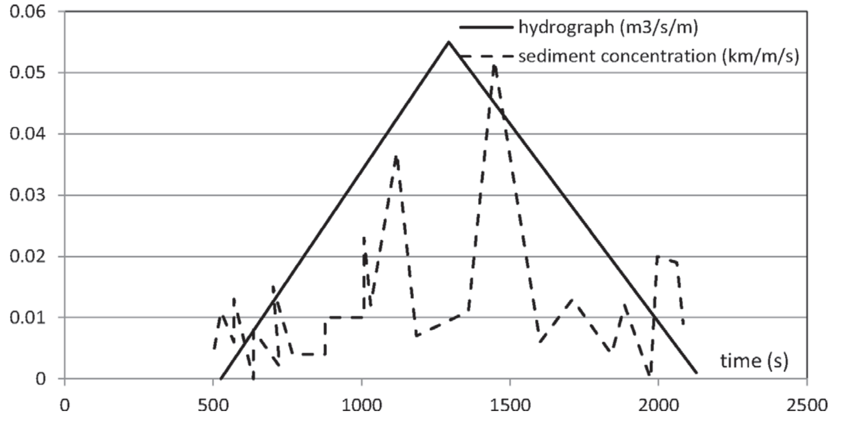


**Figure 6.**
*Sediment transport rate and flood hydrograph measured by Lee et al. [23].*

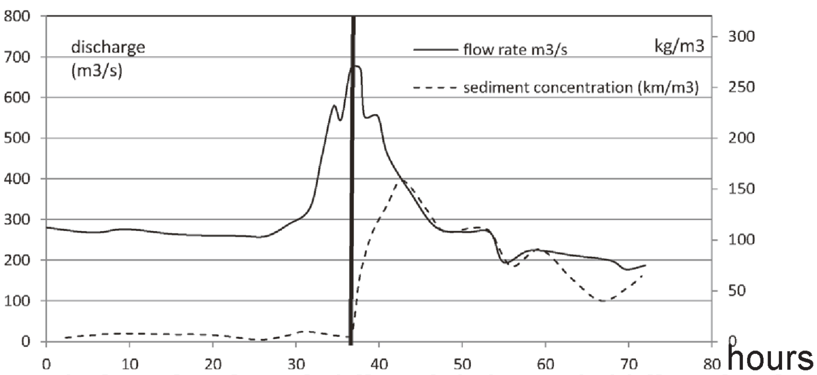


**Figure 7.**
*Measured sediment concentration over a hydrograph at Huayuankou, Yellow River from July 4–6, 2010 by Qi et al. [31].*

sediment transport (e.g., Eqs. (1)–(7) and Eqs. (34) and (35) fail to explain how the bedforms are formed, because these equations only use the streamwise parameters ($U$, $\tau$ etc.) that are constant in every cross section from upstream to downstream if the flow is steady and uniform, thus the sediment discharge in every cross section is same and no local erosion occurs, so none of them can successfully explain the formation of ripples and dunes.

However, Eqs. (14) and (22) may provide a possible explanation for the discontinuity of sediment transport from upstream to downstream. It is well known that turbulence in a steady and uniform flow is dominated by complex, multiscaled, quasi-random and organized eddies that possess both spatial and temporal coherence [43]. The velocity fluctuations are also governed by the continuity equation with the following form:

$$v' = -\int \frac{\partial u'}{\partial x} dy \tag{36}$$

The coherent events can be broadly divided into ejections ($v' > 0$ or decelerating) and sweeps ($v' < 0$ or accelerating), both of them are always alternated in space and time.

To help conceive the formation of bedforms, a flow region in **Figure 8** is divided simply into three zones, A, B and C during a short period. If the flow region B is dominated by the ejection event (denoted by "+" in **Figure 8** for upward vertical velocity), severe erosion should be observable in Zone B as Eq. (27) and **Figure 4** indicate that the upward velocity significantly promotes the sediment discharge. On the other hand, Zones A and C are dominated by the downward velocity (or negative "-" velocity), and Eq. (27) and **Figure 4** predict that the sediment carrying capacity is weaker if the vertical velocity is negative, therefore the sediment from zone B has to deposit at Zone C. It can be seen that the vertical velocity and its alternation in direction in space play a key role for the formation of dunes and ripples. The discontinuity of sediment-laden capacity along the flow direction is uneven, this triggers the formation of bedforms, once some scouring holes are formed over a flat mobile bed, erosion in these areas most likely would continue till the equilibrium condition is reached.

Alternatively, we can consider a simple model that all particles in **Figure 8** possess higher apparent density in zone A and C like iron particles (represented by dark solid circles in **Figure 8**), but the particles in zone B have lighter density (like plastic particles). All particles in zone A, B and C have the same diameter. It is understandable that a scour hole will be formed in zone B, and deposition will occur

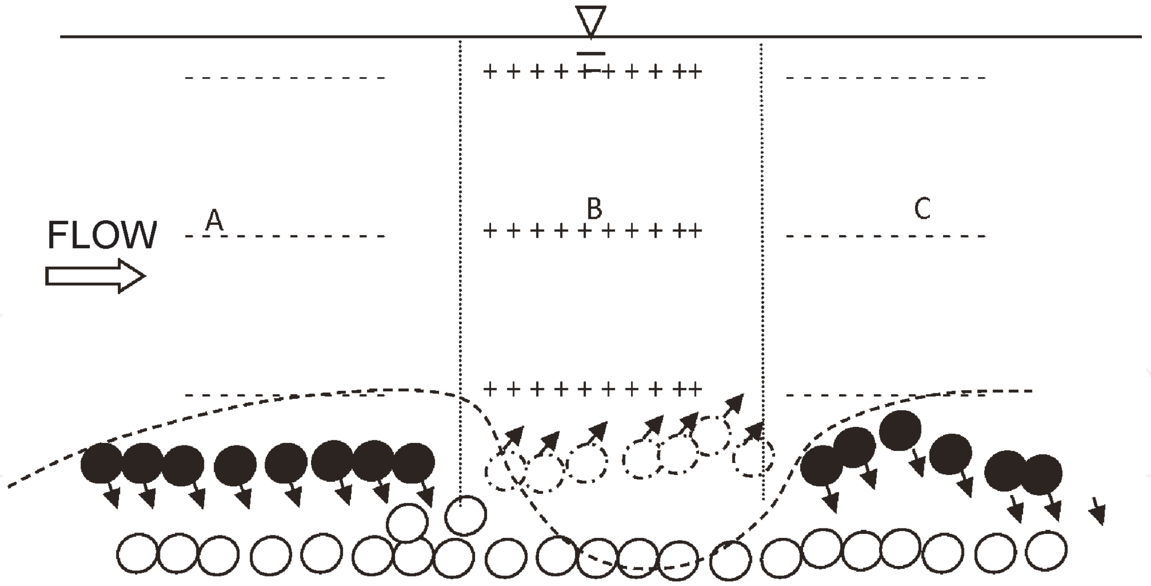


**Figure 8.**
*Relationship between the alternative vertical velocity and bedform formation, where "+" sign denotes upward velocity in region B and "-" is the downward velocity in region A and C. The dotted vertical lines denote the flow region division lines, the open circles denote the sediment particles, the solid circles denote that particles' density "becomes heavier", and dashed circles denote the "lightweight sediment", the open circles are normal sediment particles.*

at C even though the $U$ and $\tau$ remains constant in zones A to C. In other words, it can be seen that the vertical velocity and its spatial alternation play a key role for the formation of bedform. The simple model shown in **Figure 8** explains the formation of a scour hole on a flat plane that triggers the formation of bedforms. This mechanism can be extended to dune formation in deserts where the horizontal wind generates sediment transport in horizontal direct, and vertical motions yields the bedforms. The wind is accelerating along the upwind side of a dune, thus its surface is smooth, and the decelerating wind after the peak generates upward velocity, thus small holes are formed in the lee side.

By comparing the mechanism of phase lag and bedform formation discussed above, one may find that the vertical velocity is responsible for both phase lag phenomenon and bedform formation. The temporal alternation of upward and downward velocities generates the phase lag phenomenon, whilst its spatial alternation yields the bedforms. Generally speaking, we can see that the phenomena of sediment transport can be categorized into streamwise and vertical motions dominated events. Sediment transport should be expressed using variables in streamwise and vertical directions jointly.

### 6.3 Unifying mechanism of wave formation and breaking waves

Generally, all interfaces on solid–liquid, liquid–liquid, liquid-gaseous phases exist waves if there exists alterative vertical motions as shown in **Figure 8**, otherwise no waves can be observed no matter how high the velocity is if the flow is laminar. Likewise, the ocean waves between water and air are not caused by the shear stress or wind velocity on the sea surface, but the air pressure oscillation whose period should be identical to the ocean waves. In other words, turbulence is the cause of ocean waves. In summer, the heated sea surface generates an upward motion, consequently typhoons, cyclones and hurricanes can be observed. In winter, the downward cold air yields a relatively calm surface.

The existence of upward velocity can be inferred from numerous small bubbles when waves are broken. The soluble gas or air near in a lower lever like the seabed (high pressure) can be transferred to the surface (gauge pressure = 0) by the upward velocity, which causes significant pressure difference of inside and outside bubbles, consequently the bubbles are broken. In other words, from bubbles one may conclude that there is an upward velocity to transfer the bubbles from deep water to the surface, this is also true for bubbles in hydraulic jumps. It is predictable that in high speed flow, cavitation (i.e., local scour over a metal/concrete surface) can be observed when decelerating flow or the vertical flow exists. The liquefaction can be observed when the seepage velocity and particle settling velocity are in the same order of magnitude.

## 7. Conclusions

This study investigates the influence of vertical velocity induced unsteady flows on sediment transport. It is well-known that the vertical velocity is ubiquitous and it can be induced by coherent structures, non-uniformity, unsteadiness, and so on. This paper just discusses the simplest cases, i.e., the presence of vertical velocity does not significantly alter the streamwise parameters like velocity $U$ or discharge $q$, in which the rising limb or accelerating flow generates a downward velocity, but the falling limb or decelerating flow induces an upward velocity. A conceptual mathematical model is developed to account for the vertical velocity's influence on particles' critical shear stress, sediment discharge and suspension. It is found that the model can provide a qualitatively explanation to some observed phenomena. Based on this investigation, the following conclusions can be drawn:

1. The upward velocity enhances sediment mobility and downward velocity increases its stability. Mathematically the behavior of sediment transport subject to a vertical motion can be equivalently treated by the variation of apparent density. Particles become "heavier" when they experience the downward flows, this reduces the sediment transport rate. But particles become "lighter" in flows with upward velocity where the sediment discharge is increased significantly. The obtained new equation for sediment transport's apparent density is used to explain sediment transport in unsteady flows.

2. The application of Shields diagram, equations of sediment discharge and Rouse equation developed from steady flows could be extended to unsteady flows if the vertical parameter $Y$ $(= V/\omega)$ is included. The conceptual model shows that sediment is easily be transported when $Y > 0$, but difficult to move when $Y < 0$, same for the transport rate $g_t$ and Rouse number $Z$. The developed equations provide reasonably good agreement with the measured data. The condition for liquefaction can be expressed by Y = 1.

3. The mathematical model may also provide a tool to understand many odd phenomena in sediment transport like the phase lag phenomenon and bedform formation. Both are widely reported and discussed, this is the first trail to give the similarities between these two phenomena. The research shows that the temporal variation of vertical velocity results in the phase lag, and its spatial variation leads to the bedform formation.

4. In the literature, the vertical velocity is generally ignored in the measurement, which leads to that the conclusions listed above rest on the inferences of vertical velocity, not its measured values and direction. In future, systematical experiments are needed to investigate its role in order to validate the conceptual model.

## Notations

$a$ = *wave amplitude*
$a_0$ = *wave-orbital acceleration*
$C$ = averaged sediment concentration by volume
$c$ = time-average point concentration
$c'$ = fluctuation of sediment concentration
$c_f$ = friction factor
$d$ = particle diameter
$d_*$ = *dimensionless particle size*
$E$ = energy dissipated on skin friction (i.e., $\tau u_*'$)
$g$ = gravitational acceleration
$g_t$ = sediment discharge
$h$ = water depth
$H$ = wave height
$h_1$ = depth of baseflow
$h_p$ = peak flow depth of the hydrograph
$i$ = hydraulic gradient;
$k$ = constant
$k_1$ = factor
$k_0$ = wave number
$L$ = wave length
$m_1$ = coefficient
$n$ = the number of zero-downcrossing waves in the burst
$P$ = pressure
$q$ = discharge per unit width
$S$ = energy slope
$S_1$ = Sleath number
$t$ = time
$T$ = transport parameter defined by van Rijn
$T_{ZDC}$ = the period for the events
$t_d$ = duration of a hydrograph
$U$ = mean velocity
$u_*$ = shear velocity
$u_{*c}$ = critical shear velocity
$u_*'$ = shear velocity related to grain friction
$u$, $v$, $w$ = time-averaged velocity in the streamwise, vertical direction and spanwise directions
$u'$, $v'$ and $w'$ = velocity fluctuation in streamwise and vertical and spanwise directions
$U_{ZDC+}$ = the maximum current excursion in the positive direction
$U_{ZDC-}$ = the maximum current excursion in the negative direction
$V$ = vertical velocity
$U_b$ = wave-orbital speed at the bed
$V_b$ = vertical velocity at the bed
$x$ = streamwise direction
$y$ = vertical direction
$z$ = lateral direction
$Y = V_b/\omega$
$Z$ = Rouse number
$\beta$ = coefficient
$\delta$ = maximum thickness of the mobile layer
$\nu$ = kinematic viscosity

$\rho$ = fluid density
$\rho_s$ = density of sediment
$\rho_s'$ = sediment apparent density
$\sigma$ = angular frequency of waves
$\tau$ = boundary shear stress
$\tau_*$ = Shields number
$\tau_*'$ = Shields number with vertical velocity
$\tau_c$ = critical shear stress
$\tau_c'$ = critical shear stress with vertical velocity
$\omega$ = particle fall velocity
*subscribes b and t = bed load and the total load*

## Author details

Shu-Qing Yang
School of Civil, Mining and Environmental Engineering, Faculty of Engineering, University of Wollongong, Australia

*Address all correspondence to: shuqing@uow.edu.au

## References

[1] Einstein HA. Formulas for the transportation of bed load. Trans. Soc. Civ. Engrg. 1942;**107**:561-597

[2] Meyer-Peter E, Muller R. "Formula for Bed Load Transport." Proc., 2nd Meeting, Vol. Stockholm: IAHR; 1948. p. 6

[3] Yalin MS. Mechanics of Sediment Transport. Oxford, U.K.: Pergamon; 1977

[4] Engelund F, Hansen E. A Monograph on Sediment Transport in Alluvial Streams. Copenhagen, Denmark: Teknisk Forlag; 1972

[5] Ackers P, White WR. Sediment transport: New approach and analysis. J. Hydr. Div. 1973;**99**(11):2041-2060

[6] Velikanov, M. A. (1954). "Gravitational theory for sediment transport." J.of science of the Soviet Union, Geophysics, Vol. 4, (in Russian).

[7] Chien N and Wan Z. (1999), Mechanics of Sediment Transport, ASCE Press.

[8] Bagnold RA. An Approach to the Sediment Transport Problem from General Physics." Geol. Survey Professional Paper No. 422-I, U.S. Washington, D.C.: Government Printing Office; 1966

[9] Yang, C. T. (1973). "Incipient motion and sediment transport." J. Hydraul. Div., Am. Soc. Civil Engineering, 99 (10), 1679–1704.

[10] van Rijn LC. Sediment transport, Part II: Suspended load transport. J. Hydr. Engrg., ASCE. 1984;**110**(11):1613-1641

[11] Yang SQ, Tan SK. Flow resistance over mobile bed in an open-channel flow. Journal of Hydraulic Engineering, ASCE. 2008;**134**(7):937-947

[12] Yang SQ, Kim I-S, Koh DS, Song YC. Interaction of Streamwise and Wall-Normal Velocities in Combined Wave-Current Motion. China Ocean Eng. 2005;**19**(4):557-570

[13] Yang SQ, Koh SC, Kim IS, Song YC. Sediment transport capacity-an improved Bagnold formula. International Journal of Sediment Research. 2007;**22**(1):27-38

[14] Liu X.X and Chiew Y.M., (2012), "Effect of Seepage on Initiation of Cohesionless Sediment Transport". Acta Geophysica 60(6), 1778–1796. DOI: 10.2478/s11600-012-0043-7.

[15] Lee KT, Liu YL, Cheng KH. Experimental investigation of bedload transport processes under unsteady flow conditions. Hydrological Processes. 2004;**18**:2439-2454. DOI: 10.1002/hyp.1473.

[16] Nelson JM, Shreve RL, McLean SR, Drake TG. Role of near-bed turbulence structure in bed load transport and bed form mechanics. Water Resources Rese. 1995;**31**(8):2071-2086

[17] Tabarestani, M.K. and Zarrati, A.R. (2015). Sediment transport during flood event: a review, Int. J. Environ. Sci. Technol. 12:775–788, DOI 10.1007/s13762-014-0689-6

[18] Sleath JFA. Conditions for plug formation in oscillatory flow. Continental Shelf Research. 1999;**19**(13):1643-1664

[19] Francalanci S, Parker G, Solari L. Effect of seepage-induced nonhydrostatic pressure distribution on bed-load transport and bed Morphodynamics. J. Hydr. Eng., ASCE. 2008;**134**(4):378-389

[20] Cheng NS, Chiew YM. Incipient sediment motion with upward seepage.

J. Hydraul. Res. IAHR. 1999;**37**(5): 665-681

[21] Chen MS, Wartel1 S, Eck BV, Maldegem DV. "Suspended matter in the Scheldt estuary". Hydrobiologia. P. Meire & S. van Damme (eds), Ecological Structures and Functions in the Scheldt Estuary: from Past to Future. 540. 2005:79-104

[22] Wren DG, Kuhnle RA, Wilson CG. Measurements of the relationship between turbulence and sediment in suspension over mobile sand dunes in a laboratory flume. J. Geophy. Res. 2007; **112**. DOI: F03009, 10.1029/2006JF000683

[23] Cellino M, Lemmin U. Influence of coherent flow structures on the dynamics of suspended sediment transport in Open-Channel flow. Journal of Hydraulic Engineering. 2004;**130**(11):1077-1088

[24] Song T, Graf WH. Velocity and trbukence distribution in unsteady open-channel flows. J. Hydr. Eng., ASCE. 1996;**122**(3):141-154

[25] Leng X and Chanson (2016), Unsteady Turbulent Velocity Profiling in Open Channel Flows and Tidal Bores using a Vectrino Profiler. HYDRAULIC MODEL REPORT No. CH101/15, ISBN 978–1–74272-145-3, The University of Queensland, School of Civil Engineering.

[26] Schlichting H. Boundary-Layer Theory. 7th ed. New York: McGraw-Hill Book Company; 1979

[27] Kemp, P. H. and Simons, R. R.， (1982). The interaction between waves and a turbulent current:waves propagating with the current，J. Fluid Mech., 116，227 ~ 250.

[28] Kemp, P. H. and Simons, R. R.， (1983). The interaction of waves and turbulent current:waves propagating against the current，J. Fluid Mech.，130，73 ~ 89.

[29] Yang SQ, Tan SK, Wang XK. Mechanism of secondary currents in open channel flows, J. Geophysical Research. 2012;**117**:F04014. DOI: 10.1029/2012JF002510

[30] Yang SQ, Chow AT. Turbulence structures in non-uniform flows. Advances in Water Resources. 2008;**31**: 1344-1351

[31] Fredsoe, J. and Deigaard, R. (1992). Mechanics of Coastal Sediment Transport. Advanced Series on Ocean Eng., Vol. 3, World Scientific, Singapore.

[32] Nielsen P. Coastal Bottom Boundary Layers and Sediment Transport, Advanced Series on Ocean Eng. Vol. 4. Singapore: World Scientific; 1992

[33] Green MO, MacDonald IT. Processes driving estuary infilling by marine sands on an embayed coast. Marine Geology. 2001;**178**(1/4):11-37

[34] Green MO, Coco G. Review of wave-driven sediment resuspension and transport in estuaries. Reviews of Geophysics. 2014;**52**:77-117. DOI: 10.1002/2013RG000437.

[35] Yang SQ. Formula for sediment transport in rivers, estuaries and coastal waters. Journal of Hydraulic Engineering, ASCE. 2005;**131**(11):968-979

[36] Green MO. Very small waves and associated sediment resuspension on an estuarine intertidal flat. Estuarine, Coastal and Shelf Science. 2011;**93**(4): 449-459

[37] Yang SQ. Turbulent transfer mechanism in sediment-laden flow. Journal of Geophysical Research, AGU. 2007;**112**. DOI: F01005, 10.1029/2005JF000452

[38] Van de Graaff J. Sediment Concentration Due to Wave Action. Diss. Delft Univ. of Technology; 1988

[39] Rosea CP, Thorneb PD. Measurements of suspended sediment transport parameters in a tidal estuary. Continental Shelf Research. 2001;**21**: 1551-1575

[40] AL-Ragum AN. An evaluation of the rouse theory for the suspension of sand in a tidal inlet. In: PhD Thesis. UK: Univ. of Southampton; 2015

[41] Graf WH, Suszka L. Sediment transport in steep channels. J. Hydroscience., Hydr. Eng. 1985;**5**(1): 11-26

[42] Qi P, Qu SJ, Sun ZY. Suggestion on optimizing flow and sediment regulations as the operational methods of Xiaolanfdi reservoir. Yellow River. 2012;**34**(1):5-9

[43] Adrian RJ. Hairpin vortex organization in wall turbulence. Physics of Fluids. 2007;**19**:041601